2506 *J. Phys. Chem. A* **1999,** *103,* 2506−2512

Molecular Dynamics Simulations of the Solvation of Coumarin 153 in a Mixture of an Alkane and an Alcohol

F. Cichos,[†] R. Brown,[‡] U. Rempel,* and C. von Borczyskowski[§]

Institut für Physik 122501, Technische Universität Chemnitz, D-09107 Chemnitz, Germany

Received: October 14, 1998; In Final Form: February 8, 1999

Molecular dynamics simulations are applied to the preferential solvation of coumarin 153 (C153) by alcohol in an alcohol/alkane mixture, indicated by recent steady-state and time-resolved spectroscopic measurements.[1] Simulations of weakly polar mixtures are done for the ground and the excited states of C153, using detailed models of the dye. Solvation of C153 by the alcohol is almost negligible in the ground state, with correspondingly little effect on the absorption spectrum of the dye, whereas preferential solvation of the excited state leads to a large solvation shift of the fluorescence spectrum, in agreement with experiment. The simulated solvation shell and its dynamics are described and related to the solvation shifts.

1. Introduction

Understanding solvation and the dynamics of solvent motion has been the goal of many experimental and theoretical studies during the last 40 years.[2−6] A common way to explore these processes is to study the Stokes shift of the emission of a probe solute.[7,8] The shift is due to the reorganization of the solvent molecules around the solute after the redistribution of charges on the solute by optical excitation. Steady-state and time-resolved fluorescence spectroscopy provide information on the solute−solvent interactions and on the solvent dynamics. Most of the time-resolved experiments performed so far concentrate on the behavior of pure polar[9−11] or nonpolar solvents,[12] while only little work was done on mixed solvents.[13] Two reasons for studying solvation in mixtures are that translational relaxation of the solvent may be significant (whereas rotation predominates in pure polar solvents[7,8]) and that solvation in the case of preferential solvation in weakly polar mixtures might be attributable to the relaxation of a single solvation shell.

Computer simulations have already contributed to our understanding of molecular aspects of solvent motion. Early molecular dynamics (MD) work in this respect was done on simple model systems consisting of spherical or diatomic solutes and of simplified solvent molecules.[14−17] Semiempirical studies now provide good molecular models for polyatomic solutes, such as those mostly used in experiments. Thus the gap between simulation and experiment is being reduced and MD simulations are useful for understanding solvation dynamics of large dyes, e.g., C153,[18] AMBO[19] or 3-methylindole,[20] and coumarin 120.[21] Thus, one of the main conclusions of these studies is that the solvent response to the jump in charge on the dye molecule on excitation is linear although the jump of the dipole of the dye may be of the order of 20 D. We employed MD simulations with a detailed model of C153 to explore the solvation of this solute in a mixture of methanol and hexane molecules. A series of ground- and excited-state equilibrium simulations of C153 was undertaken in order to determine the structure of the solvation shell and to calculate the shift and broadening of absorption and emission spectra compared to those in the pure nonpolar solvent. The results are in fair agreement with our experimental data taken from steady-state absorption and time-resolved emission data.[1]

2. Method and Analysis

2.1. Molecular Models and Simulations. Solutes and solvents employed in this work are treated as rigid bodies. Data on all systems were accumulated in a NVT ensemble after a period of equilibration at constant pressure, using the Berendsen thermostat and barostat.[22] Solvation of C153 in the methanol/hexane mixtures was studied in equilibrium simulations with the excited and ground states of C153. Each simulation covered 2.5 ns with a 5 fs time step. A 12 Å cutoff was applied to both electrostatic and short-range forces, the cutoff to the former being applied to a sum of interactions between neutral charge groups. The electrostatic interactions were probed every 10 steps and the configuration every 50 steps.

The experimental data were taken from ref 1 at a polar mole fraction of 0.044, which corresponds to the value used in the simulations. Results are shown for one C153 molecule in solution in 216 hexane molecules and 10 methanol molecules.

The intermolecular forces are described by Lennard-Jones and Coulomb potentials. The solvents, methanol and hexane, were modeled with the OPLS parametrization of Jorgensen,[23,24] without change in the case of hexane. The united atom model of the methanol methyl group interactions was maintained but the total mass was distributed on all atoms, making rotation about the C−O axis slower. The moment of inertia for a motion around the C−O axis of methanol is thus altered by a factor of 5. Structural and dynamical properties of the solvent models were checked in simulations of the pure solvents and compared to results in the literature.[23,24] Methanol exhibits characteristic pair correlations reflecting the hydrogen bonding in this alcohol. Maxima of the O−H correlation were found at 1.8 and 3.2 Å, and the O−O correlation showed maxima at 2.7 and 4.8 Å. Reference data in refs 24−26 place these maxima at 1.82 and

---

* Author to whom correspondence should be addressed. E-mail: rempel@physik.tu-chemnitz.de.

[†] E-mail: cichos@physik.tu-chemnitz.de.

[‡] Centre de Physique Moléculaire Optique et Hertzienne, u.m.r. 5798 du C.N.R.S. et de l'Université Bordeaux I, 33405 Talence Cedex, France. E-mail: brown@yak.cpmoh.u-bordeaux.fr.

[§] E-mail: borczysk@physik.tu-chemnitz.de.

10.1021/jp984080t CCC: $18.00

3.3 Å for the O−H and at 2.75 and 4.8 Å for the O−O correlations. The molecular volume of methanol was calculated to be 68.3 Å^3 which is close to the experimental value of 67.2 Å^3.[27] Hexane shows no distinct pair correlations. The rigid molecule occupies a volume of 213.8 Å^3 compared to the experimental value of 216.7 Å^3.[27]

Preferential solvation is caused by the fact, that the two components of the solvent mixture have strongly different interactions with the solute. As this interaction may show specific site−site interactions such as hydrogen bonding,[28] it is important to use an appropriate set of potential parameters, including a charge model and a detailed set of Lennard-Jones parameters. The quality of the model may then be judged by comparison of calculated and experimental emission and absorption shifts in the pure polar solvent.

The charge model and the geometry of C153 were obtained from semiempirical calculations with MOPAC.[29] The structure of C153 optimized in MNDO ground-state calculations was in agreement with ref 18. The Lennard-Jones parameters were redefined compared to ref 18 to use a more detailed description of specific site−site interactions between C153 and the solvent atoms. Three types of carbon atoms were defined depending on their position and bonding properties (carbon double-bonded with no hydrogen attached (a), carbon double-bonded with one attached hydrogen (b), carbon with two attached hydrogens (c). The parameters for the carbons (a, b), oxygen, and nitrogen atoms were taken from the gromos87 force-field[30] while for the carbon (c) those of the OPLS force field[23,24] were used. The hydrogen atoms have no Lennard-Jones interaction potential. The fluorine parameters were taken from ref 18. The charges for the ground and excited state were obtained from MNDO and AM1 calculations using Coulson population analysis. The dipole moments obtained for the ground and excited state of C153 from these calculations are 5.9 and 11.7 D with the MNDO Hamiltonian, comparable to the values in ref 18. The AM1 Hamiltonian leads to dipole moments of 6.6 and 13.7 D. The experimental values of 6.6 D[31] for the ground state and 15 D[32] for the excited state favor the use of the AM1 charge model. This choice is additionally supported by MD simulations of C153 in pure methanol using both charge models. The MNDO charges resulted in a shift of −800 cm^{-1} for absorption and −1500 cm^{-1} for the emission. The AM1 charges caused an absorption shift of −1000 cm^{-1} and an emission shift of −3170 cm^{-1}. The latter are closer to the experimental absorption and emission shifts of 1960 and 3760 cm^{-1},[1] respectively. It should be noted that the experimental and simulated data refer to the spectra in hexane which we consider to be a reasonable estimation of the effect of dispersion interaction and of polarizability of the solvent in the dilute alcohol mixtures, but only an approximate estimation of these effects in pure alcohols.

2.2. Calculation of the Spectra. Shift and broadening of the electronic spectra of a solute molecule in a solvent are caused by the difference in solute−solvent dispersion, induction, and permanent electrostatic interactions, between the ground and excited states.[33]

While in a pure nonpolar solvent dispersion and induction mainly determine these changes, additional polar solvent molecules will contribute mainly electrostatic interactions with the solute. The jump of this additional electrostatic interaction due to different solute atomic charges when switched from the ground to the excited state leads to a spectral shift and broadening. For example, the electrostatic absorption shift is

$$\Delta W_{0\to1} = \sum_i (q_i^1 - q_i^0) V(\vec{r}_i) \tag{2.1}$$

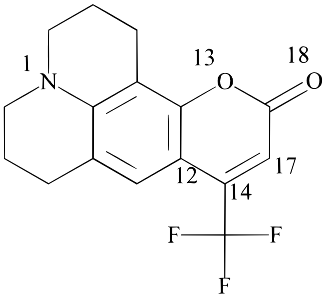

Figure 1. Structure of C153 with numbering of individual atoms.

where the sum is over all solute atoms *i* and *V* is the electrostatic potential created by the solvent initially in dynamical equilibrium with the solute ground state. These interactions are inhomogeneously distributed due to varying solute−solvent interactions of different solute molecules, leading to the broadening of the absorption or emission band. A similar expression represents the emission shift $\Delta W_{1\to0}$. Since we are interested in the effect of the electrostatic interactions in dilute polar mixtures, the dispersion and induction effects are estimated from the spectrum of the solute in pure hexane. The quality of this estimation will be discussed in section 4. The absorption and fluorescence spectra in the mixture are then described by a convolution of the solute absorption (subscript A) or emission (F) line shape function with the inhomogeneous distribution of the electrostatic solvation shift $p(\Delta W)$.[34]

$$A_M(h\nu) \propto \nu \int g_A(h\nu - \Delta W_{0\to1}) p_A(\Delta W_{0\to1})\, d(\Delta W_{0\to1}) \tag{2.2}$$

$$F_M(h\nu) \propto \nu^3 \int g_F(h\nu - \Delta W_{1\to0}) p_F(\Delta W_{1\to0})\, d(\Delta W_{1\to0}) \tag{2.3}$$

The line shape functions $g_{A,F}(h\nu)$ are obtained from the solute absorption and emission spectrum in pure hexane by $g_A(\nu) = A(\nu)/\nu$ and $g_F(\nu) = F(\nu)/\nu^3$, where as in eq 2.2 and 2.3 the factors ν and ν^3 account for the change of absorption or emission probability with photon energy. As the MD simulations include only one solute molecule, the distribution of the ensemble is replaced by a time distribution of ΔW for this single molecule. The simulation is performed with C153 in its electronic ground state to yield the $p_A(\Delta W_{0\to1})$ relevant for absorption. At regular intervals the electrostatic contribution to the solvation is also evaluated with the charges of C153 switched to their excited-state values, without performing a simulation step. The resulting electrostatic energy difference for the excited and ground state is $\Delta W_{0\to1}$. The simulation then resumes with the ground-state charges. The calculation of $p_F(\Delta W_{1\to0})$ for emission is done correspondingly in the excited state.

3. Results

3.1. Structure of the Solvation Shell. The composition of the solvation shell is monitored by the solvation number, defined here as the number of MeOH molecules within a certain distance of at least one C153 atom. The separation is reckoned to the center of geometry of the MeOH molecule. Figure 2 shows the distribution of solvation numbers (separations up to 4 Å) of C153 in a MeOH/hexane mixture (mole fraction $x_P = 0.044$), averaged over 2.5 ns. These probabilities correspond to the average portion of dye molecules in an experimental ensemble with given solvation number. In the ground state, S_0, the most probable situation (55%) is to find no MeOH molecule within 4 Å of the dye. Nevertheless, 45% of the C153 molecules have

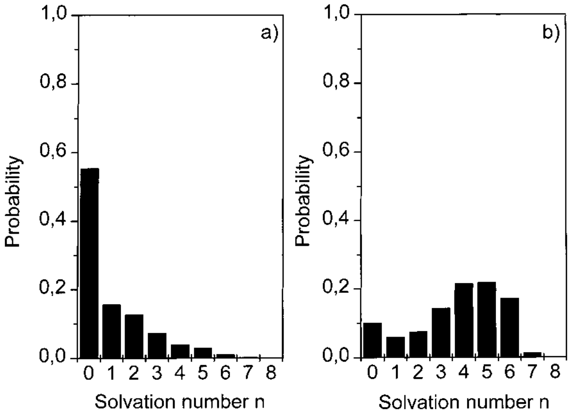

Figure 2. Distributions of MeOH solvation numbers (within 4 Å) of C153 in a MeOH/hexane mixture ($x_P = 0.044$) (a) ground-state S_0, (b) excited-state S_1.

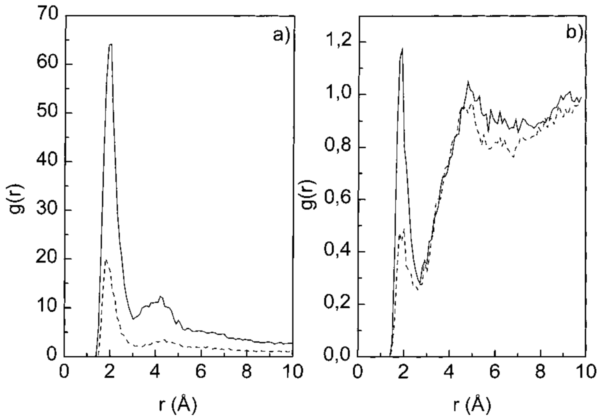

Figure 3. (a) O18(C153)-H(MeOH) correlation function for C153 in (a) the MeOH/hexane mixture (ground-state, dashed; excited-state, full line), (b) O18(C153)-H(MeOH) correlation function for C153 in pure MeOH (ground-state, dashed; excited-state, full line).

one or more MeOH molecules closer than 4 Å so that preferential solvation exists in the ground state of C153 too, but it is rather weak (see also the correlation functions below). The most probable configuration for the C153 molecule in the exited state S_1 is to have 4 or 5 molecules within 4 Å. About 40% of the dye molecules in an ensemble would have that solvation number, showing the increased preferential solvation in the excited-state S_1 due to the stronger electrostatic interaction, compared to S_0.

Pair correlation functions were determined for the C153 atoms O18, N1, and C14 with the hydroxyl hydrogen of the MeOH. The O18 and N1 atoms are of interest since they are able to accept hydrogen bonds donated by the hydroxyl hydrogen of the MeOH. The C14 atom has the strongest charge change (−0.2531 e) on excitation of the dye. For comparison, the results for a simulation of C153 in pure MeOH are also shown.

Figure 3a shows the correlation function for the O18−H distance for both electronic states of C153. A strong first maximum at about 1.8 Å [$g(1.8) = 20$] in S_0 and 1.9 Å [$g(1.9) = 64$] in S_1 is visible. Taken with the first maximum in the O18−O correlation (not shown) it is characteristic of a hydrogen bond. In comparison, the O18−H hydrogen bond for C153 in pure MeOH is weak (Figure 3b: note the different vertical scale as compared to Figure 3a). The first maximum in the ground-state S_0 is at 1.9 Å [$g(1.9) = 0.49$]. The value of the correlation function at 1.9 Å increases in the excited-state S_1 to $g(1.9) = 1.17$. O13 also shows a hydrogen bond to MeOH (plots not shown).

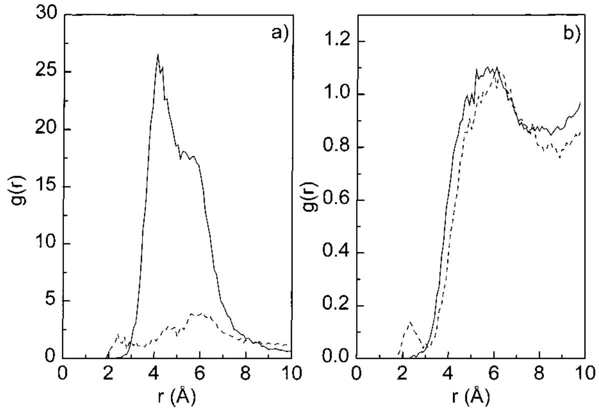

Figure 4. (a) N1(C153)-H(MeOH) correlation function for C153 in the MeOH/hexane mixture (ground-state, dashed; excited-state, full line), (b) N1(C153)-H(MeOH) correlation function for C153 in pure MeOH (ground-state, dashed; excited-state, full line).

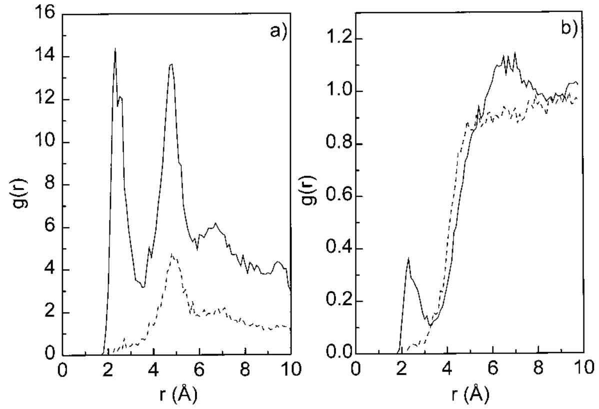

Figure 5. (a) C14(C153)-H(MeOH) correlation function for C153 in the MeOH/hexane mixture (ground-state, dashed; excited-state, full line), (b) C14(C153)-H(MeOH) correlation function for C153 in pure MeOH (ground-state, dashed; excited-state, full line).

The N1−H correlation of the MeOH/hexane mixture, shown in Figure 4a, displays no signs of a hydrogen bond. The correlation function in the ground state is almost structureless with a maximum at 6 Å [$g(6) = 4$, hydrogen sitting over other solute atoms]. In the excited state, a broad peak with a maximum at 4.2 Å [$g(4.2) = 26.5$] is found. Because of the decreased negative charge on N1 in the excited state (S_0: −0.2886 e, S_1: −0.1305 e) the hydroxyl hydrogen moves away from the nitrogen. The same behavior is found for C153 in pure MeOH (Figure 4b). Here a small peak at about 2.3 Å in the ground state shows a weak tendency of the N1 atom to accept a hydrogen bond. Shielding of N1 by surrounding C153 atoms explains the difference between N1 and O18 although the negative charges on these sites in the ground state are comparable.

The C14−H correlation function (Figure 5) in the mixture has a peak at 4.8 Å [$g(4.8) = 4.8$ for S_0], due to the hydrogen bond at the O18 (and O13) atom (C14−O13 distance 2.8 Å, C14−O18 distance 3.6 Å). In the excited state of C153 an additional peak at 2.3 Å appears and is attributed to a specific bond. The cause of this peak is the increased negative charge of the C14 atom in the excited state (S_0: −0.0341 e, S_1: −0.2872 e). Corresponding behavior is observed for C153 in pure MeOH but with a weaker tendency to form the specific bond. The maximum here is at 2.3 Å [$g(2.3) = 0.36$] in the excited state.

The MeOH−MeOH correlations in the mixture were calculated. Strong clustering of MeOH molecules in the mixture is

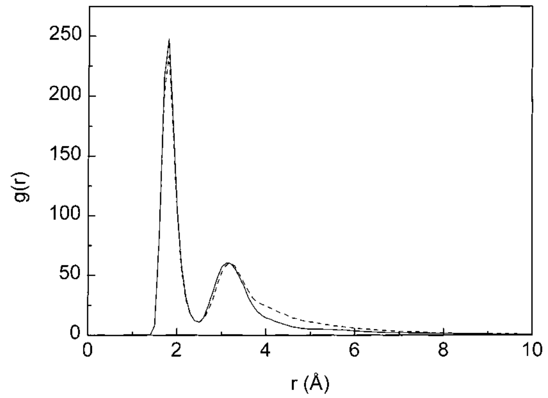

Figure 6. O−H correlation function for MeOH in the C153/MeOH/hexane mixture (ground-state of C153, dashed line; excited-state of C153, full line).

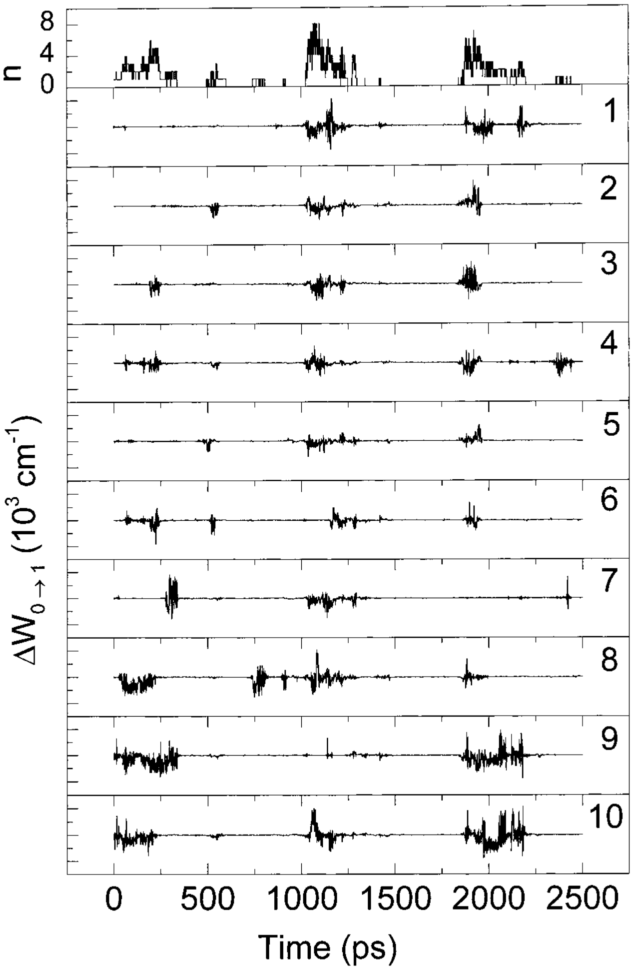

Figure 7. Solvation number (within 4 Å) and electrostatic solvation shifts $\Delta W_{0\to1}$ of C153 contributed by each MeOH molecule (numbered 1−10) from a ground-state equilibrium simulation of C153 in a MeOH/hexane mixture with an alcohol mole fraction of $x_P = 0.044$. The spacing of the major tick marks in the lower diagrams is 1000 cm^{-1}. The periods of almost straight lines correspond to 0 cm^{-1}.

observed (Figure 6). Differences between correlations in both electronic states of the dye are small. Mainly the second peak of the correlation function is narrower in the excited state than in the ground state, being an effect of the stronger preferential solvation in the excited state, which brings most of the MeOH close together near the dye.

3.2. Calculated Spectra. *Absorption.* Figure 7 shows in the lower diagrams the contribution of each MeOH molecule to the electrostatic solvation shift energy $\Delta W_{0\to1}$ obtained from ground-state simulations. The plots display for each MeOH several regions of strong fluctuations from 800 to −800 cm^{-1}, interrupted by periods with no interaction. These periods are correlated because of clustering of the alcohol, e.g., molecules 1−5 between 1 ns and 2 ns. The sum over all single MeOH contributions ranges from 1000 to −1500 cm^{-1}. As shown in Figure 7 in the first diagram, the strong fluctuations correlate with periods where the solvation number within 4 Å is nonzero. It varies during these periods mostly between 1 and 5 (with a few cases where it goes up to 7 or 8 or down to 0). The average solvation number over the whole simulation is 1.06. Obviously, there is no strong binding of methanol to the coumarin and therefore the coumarin−methanol interaction is determined by translational motion. The histogram of the overall $\Delta W_{0\to1}$ yields the inhomogeneous absorption profile (Figure 8a). This distribution shows a very sharp maximum at 0 cm^{-1} and a long flat tail down to −1000 cm^{-1}. The absorption spectrum resulting from a convolution of the simulated shifts with the experimental absorption spectrum in pure hexane (according to eq 2.2) is shown in Figure 8b. The spectrum is centered at 25760 cm^{-1} and has a width (standard deviation) of 1990 cm^{-1}. It is shifted −200 cm^{-1} to the red and about 20 cm^{-1} broader compared to the spectrum in pure hexane. The experimentally observed red-shift at an alcohol mole fraction of $x_P = 0.044$ is −340 cm^{-1} (center 25620 cm^{-1}, width 2260 cm^{-1}).

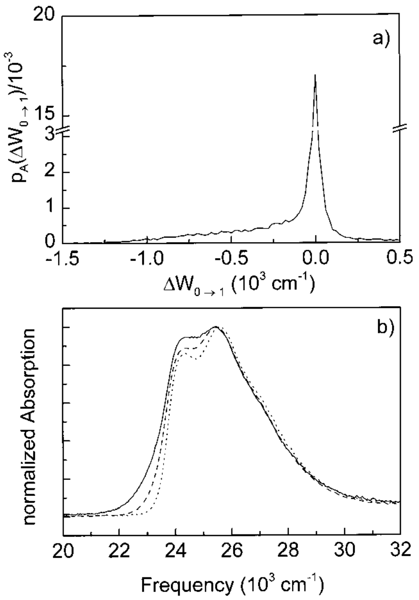

Figure 8. Spectral distribution (a) for the absorption of C153 derived from the shifts in Figure 7. Absorption spectrum ((b), dashed line) calculated from the distribution in (a) with the reference spectrum (dotted line) of C153 in hexane and experimental spectrum (solid line: $x_P = 0.044$[1]).

Emission. In contrast to the ground state (Figure 7) the contributions to the electrostatic solvation shift $\Delta W_{1\to0}$ calculated from the excited-state simulation show much longer periods of interaction for the MeOH molecules (Figure 9, lower diagrams). The energy varies from 300 to −1500 cm^{-1}. The clustering of the alcohol in the alkane again explains why the interactions with different molecules are correlated, e.g., numbers 1, 5, 7, and 9. The sum of all interactions ranges from 300 to −3500 cm^{-1}. Accordingly, the solvation number is nonzero almost permanently (Figure 9, upper diagram) with average 3.7. The histogram (inhomogeneous fluorescence shift) in Figure 10a is now dramatically red-shifted and broadened. The emission spectrum calculated from the simulation is plotted in Figure

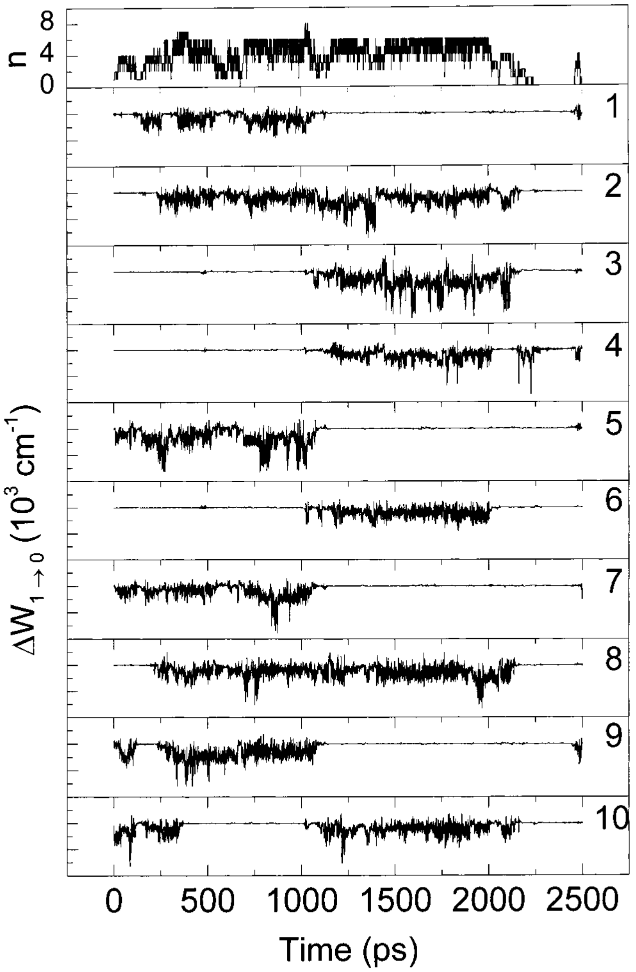

Figure 9. Solvation number and electrostatic solvation shift $\Delta W_{1\rightarrow 0}$ of C153 due to each MeOH molecule (numbered 1−10) from an excited-state equilibrium simulation of C153 in the MeOH/hexane mixture. The spacing of the major vertical tick marks in the lower diagrams is 1000 cm^{-1}.

10b together with the reference spectrum of C153 in pure hexane (dashed line, center 21870 cm^{-1}, width 1400 cm^{-1}). The spectrum is centered at 20400 cm^{-1} and has a width of 1590 cm^{-1}, to be compared with the experimental values 19920 and 1640 cm^{-1}. The experimental spectrum was obtained from the equilibrated region of time-resolved measurements (i.e., after the time-dependent Stokes shift is completed). Steady-state emission spectra are not suitable for comparison as they include fluorescence from molecules that are not equilibrated right after excitation, which cause an additional broadening on the short-wavelength side of the spectrum.[1] This broadening effect is especially important when the solvent relaxation is close to the emission lifetime as observed in such mixtures.

4. Discussion

The experimental results in ref 1 suggest that C153 in alcohol/alkane mixtures is preferentially solvated by the alcohol. In addition the preferential solvation is stronger in the first excited-state S_1 of the dye than in S_0. The simulations clearly confirm this experimental result and show that S_1 involves a solvation number about 3.5 times larger than S_0. The correlation functions indicate that interactions between specific pairs play an important role in the formation and stability of the solvation shell. The hydrogen bond between the C153 O18 atom and MeOH is a main reason for the formation of preferential solvation in this mixture. In contrast to the obvious strong influence of the C153 molecule on its surrounding in the mixture (Figure 3a), the solvation shell of C153 in pure MeOH is rather unaffected by specific solute−solvent bonds (Figure 3b). There the MeOH surrounding the first solvation shell lowers the barriers for the dissociation of solute−solvent bonds and therefore the coumarin only weakly disturbs the MeOH structure.

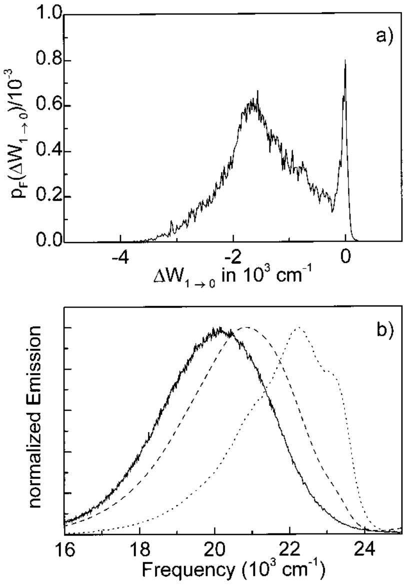

Figure 10. Spectral distribution (a) for the emission of C153 derived from the differential interaction energy from Figure 9. Emission spectrum ((b), dashed line) calculated from the distribution in (a) with the reference spectrum (dotted line) of C153 in hexane and the experimental spectrum (solid line, $x_P = 0.044$[1]).

Despite this importance of hydrogen bonds for preferential solvation they should have almost no effect (besides a lowering of the mobility of the bound MeOH) on the solvation dynamics since there is no direct change in the strength of the hydrogen bond observed. The charge jump on the O18 atom upon excitation is less than 10^{-2} *e*. The increased O18−H correlation in the excited state is an effect of the charge transfer from the N1 to the C14/C17 position and thus the increased attractive potential for positive charges in the region of O18. The same argument should hold for C153 in pure MeOH.

Since the electronic states of the coumarin dye involve a different number of solvent molecules in the surroundings and because the preferential solvation in the ground state is weak, the solvation dynamics in dilute polar solutions will mainly reflect translational diffusion as determined in ref 1. Figures 6, 7, and 9 indicate that a clustering of methanol molecules will strongly influence this translational diffusion. Rotational motions are expected to play a more important role when the polar solvation of the dye molecules in the ground state increases, e.g., at higher methanol concentrations.

The MD simulations are reasonably successful in determining the steady-state spectra of C153 in mixtures of hexane and methanol. Specially the spectral properties stemming from the difference in preferential solvation of the solute ground and excited states are well represented by the simulations. The main discrepancy is an underestimation of the solvent shifts. Summarizing the results for an alcohol concentration of $x_P = 0.044$ the calculated absorption spectrum reproduces 59% of the experimental absorption shift, while the calculated emission spectrum shows 75% of the experimental emission shift. The same order of magnitude of deviation is observed for C153 in pure methanol (absorption: 51%, emission: 84%). That in the

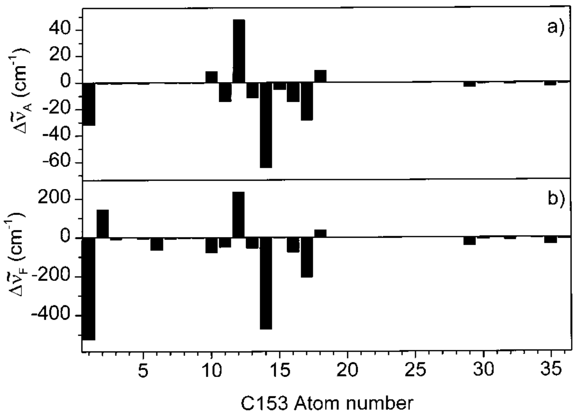

Figure 11. Contributions of the charge jump on the C153 atoms to the shift of the absorption (a) and emission (b) spectrum of C153 in the MeOH/hexane mixture.

real (or simulated) system one C153 molecule might be able to fix more than the 10 methanol molecules in our finite simulation, though possible, is therefore not the main cause of the discrepancy. A further source of inaccuracy is neglect of the polarizability of the solvent, which should actually lead to a small blue-shift in the mixture, since hexane has a greater electronic polarizability (11.9 Å^3 [27]) than methanol (3.3 Å^3 [27]). An estimation (using classical continuum reaction field formulas) of the interaction due to induced dipole moments in hexane and methanol shows that the shift is about 100 cm^{-1} smaller for methanol. Since the dispersion interaction change is approximately of the same order of magnitude,[32] we estimate that induction and dispersion interaction in the mixture should lead to a blue-shift of about 200 cm^{-1} of the calculated spectra. We think the main source of the deviations is the neglected electronic polarizability of the dye molecule itself. Electrooptical measurements on C120 in different solvents[35] show that an additional dipole moment of 1−3 D is induced by the surrounding polar solvent. The larger coumarin dipole moment would thus cause a larger red-shift. An estimation of the absorption or emission shift with an additional induced dipole moment of 3D results in a 1.45 and 1.2 times larger absorption/emission shift than without the solute polarizability. Consideration of the solute polarizability as in refs 20 and 21 is therefore necessary. In addition the simulations neglect inner degrees of freedom for the molecules. Flexible models would change the mobility of the molecules (e.g., the diffusion coefficient[36]) and thus change the stability of preferential solvation.

A final question is whether the expense of detailed atomic simulations is justified for solvation calculations, in which it might be expected that thermal agitation would blur the fine details of atom−atom interactions. Indeed, analyzing the contributions of single coumarin atoms to the absorption and emission shift leads to the result that the largest effects on the spectra (Figure 11) come from the four C153 atoms with the strongest charge jump (N1, C12, C14, and C17). Since they almost lie on a straight line, the charge jump between S_0 and S_1 and the interactions which cause the spectral shift, are nearly dipolar. Thus, a simple dipole model of C153 might be thought to be adequate. In fact, analysis of the contribution of MeOH molecules in different positions (see as an example configuration Figure 12) with respect to the C153 shows that while the charge jump on the O18 atom is negligible, a MeOH in a hydrogen-bonding position contributes about −480 cm^{-1} on average to the emission and −260 cm^{-1} to the absorption shift. Therefore, the solute−solvent hydrogen bond to O18, though not directly involved in the shift, is important for absorption and emission shifts in such mixtures as an anchor for methanol close to atoms involved in the charge transfer. A specific bond at the C14 atom in the excited state contributes about −1000 cm^{-1} to the emission shift but is less effective due to its lower stability (see

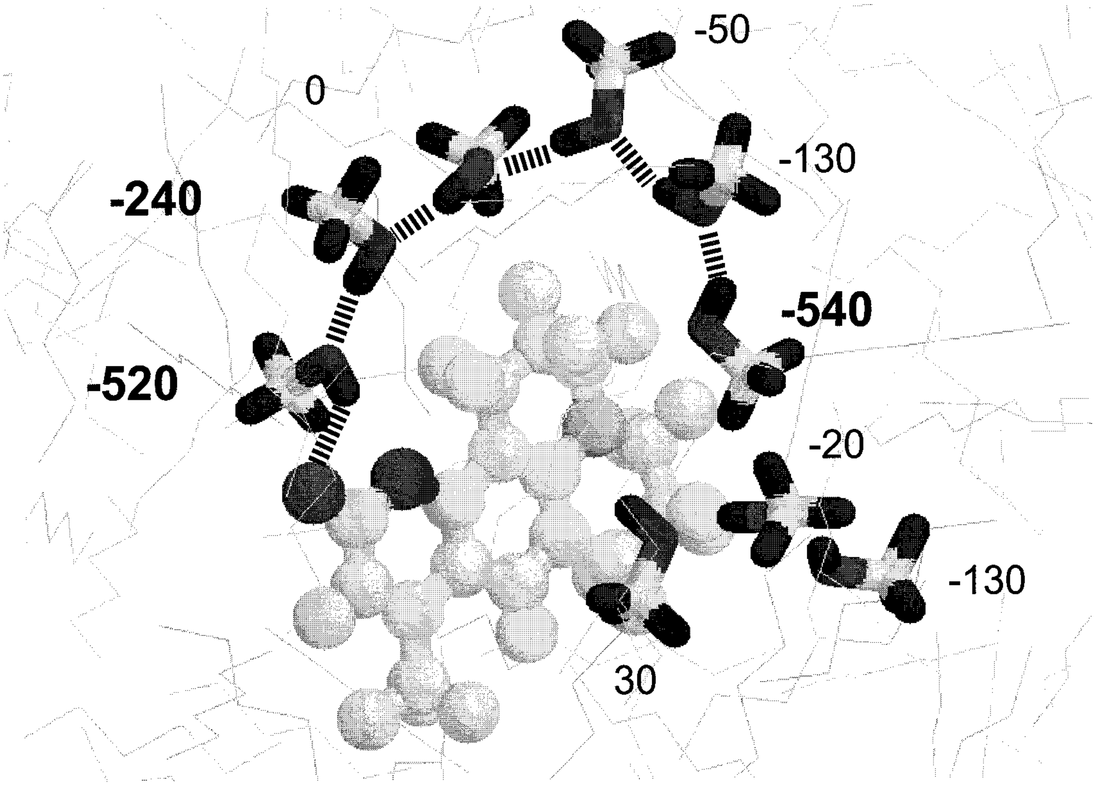

Figure 12. Sample configuration for the excited state of C153 in the MeOH/hexane (hexane shown in outline) mixture. Hydrogen bonds are shown hatched. The numbers indicate the individual contributions of the MeOH molecules to the emission shift (in cm^{-1}).

the pair correlation Figure 5). Further, the clustering of MeOH molecules binds additional MeOH to the solvation shell (Figure 12), causing additional shift and broadening of the spectra, even if their direct interaction with C153 is comparable or below thermal energy. Thus, even though the charge transfer in the electronic transition is dipolar in character, the multipole character of the individual states is important for the correct understanding of the experimental results.

Conclusion

The present molecular dynamics simulations of the solvation of coumarin 153 in a methanol/hexane mixture connect structural and spectral properties in this system. The results, which are in fair agreement with experimental data in ref 1, confirm the strong preferential solvation of coumarin 153 by methanol in the excited state and point out that such mixtures of polar and nonpolar solvents may be valuable for studying specific solute–solvent interactions. On the other hand, the simulations show that dilute polar/nonpolar mixtures can have quite different solvation shells and dynamics from the pure polar solvent, and are not necessarily representative of the dynamics of the first solvation shell in the polar solvent. It would be interesting to examine this point for less strongly structured solvents than methanol.

Acknowledgment. This work was supported by the Deutsche Forschungsgemeinschaft within the Schwerpunkt “Schnelle molekulare Prozesse in Flüssigkeiten”, by the Groupement de Recherche 1017 du C.N.R.S. and by a scholarship to F.C. of the Freistaat Sachsen. R.B. acknowledges use of the Cray T3E parallel computers of the Idris and the Pôle de Modélisation Numérique Intensive de l'Université de Bordeaux I. All simulations were performed with the dl-poly molecular dynamics suite, courtesy of C.C.L.R.C. Daresbury, U.K.[37]

References and Notes

(1) Cichos, F.; Willert, A.; Rempel, U.; von Borczyskowski, C. *J. Phys. Chem. A* **1997**, *101*, 8179.
(2) Mataga, N.; Kaifu, Y.; Koizumi, M. *Bull. Chem. Soc. Jpn.* **1956**, *29*, 465.
(3) Bilot, L.; Kawski, A. Z. *Naturforsch.* **1962**, *17a*, 621.
(4) Maroncelli, M.; MacInnis, J.; Fleming, G. R. *Science* **1989**, *243*, 1647.
(5) Stratt, R. M.; Maroncelli, M. *J. Phys. Chem.* **1996**, *100*, 12981.
(6) Ladanyi, B. M.; Maroncelli, M. *J. Chem. Phys.* **1998**, *109*, 3204.
(7) Reichardt, C. *Solvents and Solvent Effects in Organic Chemistry*; VCH: Weinheim, 1990.
(8) Maroncelli, M.; Fleming, G. R. *J. Chem. Phys.* **1987**, *86*, 6221.
(9) Kahlow, M. A.; Kang, T. J.; Barbara, F. *J. Chem. Phys.* **1988**, *88*, 2372.
(10) Rosenthal, S. J.; Xie, X.; Du, M.; Fleming, G. R. *J. Chem. Phys.* **1991**, *95*, 4715.
(11) Horng, M. L.; Gardecki, J. A.; Papazyan, A.; Maroncelli, M. *J. Phys. Chem.* **1995**, *99*, 17311.
(12) Berg, M. *Chem. Phys. Lett.* **1994**, *228*, 317.
(13) Petrov, N. Kh.; Wiessner, A.; Fiebig, T.; Staerk, H. *Chem. Phys. Lett.* **1995**, *241*, 127.
(14) Carter, E. M.; Hynes, J. T. *J. Chem. Phys.* **1991**, *94*, 5961
(15) Maroncelli, M. *J. Chem. Phys.* **1991**, *94*, 2084.
(16) Fonseca, T.; Ladanyi, B. M. *J. Phys. Chem.* **1991**, *95*, 2116.
(17) Ladanyi, B. M.; Sratt, R. M. *J. Phys. Chem.* **1996**, *100*, 1266.
(18) Kumar, P. V.; Maroncelli, M. *J. Chem. Phys.* **1995**, *103*, 3038.
(19) Brown, R. *J. Chem. Phys.* **1995**, *102*, 9059; Brown, R. *J. Chem. Phys.* **1995**, *103*, 5868.
(20) Muino, P. L.; Callis, P. R. *J. Chem. Phys.* **1994**, *100*, 4093.
(21) Ando, K. *J. Chem. Phys.* **1997**, *107*, 4585.
(22) Berendsen, H. J. C.; Postma, J. P. M.; van Gunsteren, W.; DiNola, A.; Haak, J. R. *J. Chem. Phys.* **1984**, *81*, 3684.
(23) Jorgensen, W. L.; Madura, J. D.; Swenson, C. J. *J. Am. Chem. Soc.* **1984**, *106*, 6638.
(24) Jorgensen, W. L. *J. Phys. Chem.* **1986**, *90*, 1276.
(25) Narten, A. H.; Habenschuss, A. J. *J. Chem. Phys.* **1984**, *80*, 3387.
(26) Wertz, D. L.; Kruh, R. K. *J. Chem. Phys.* **1967**, *47*, 388.
(27) *Handbook of Chemistry and Physics*; Lide, D. R., Ed.; CRC Press: Boston, **1990**.
(28) Chapman, C. F.; Fee, R. S.; Maroncelli, M. *J. Chem. Phys.* **1995**, *99*, 4811.
(29) Dewar, M. J. S.; Thiel, W. *J. Am. Chem. Soc.* **1977**, *99*, 4899.
(30) van Gunsteren, W. F.; Berendsen, H. J. *C. Groningen Molecular Simulation Library Manual*; Biomos: Groningen, The Netherlands, 1987.
(31) Moyland, C. R. *J. Phys. Chem.* **1994**, *98*, 13513.
(32) Baumann, W.; Nagy, Z. *Pure Appl. Chem.* **1993**, *65*, 1729.
(33) Matyushov, D. V.; Schmid, R.; Ladanyi, B. M. *J. Phys. Chem.* **1997**, *101*, 1035.
(34) Mazurenko, Yu. T. *Opt. Spectrosc. (USSR)* **1980**, *40*, 388.
(35) Nemkovich, N. A.; Reis, H.; Baumann, W. *J. Lumin.* **1997**, *71*, 255.
(36) Padilla, P.; Toxvaerd, S. *J. Chem. Phys.* **1991**, *95*, 509.
(37) Forester, T. R.; Smith, W. The DL_POLY_2.0 User Manual, CCLRC: Daresbury Laboratory, Warrington WA4 4AD, U.K.